Energy 141 (2017) 1829–1835

Contents lists available at ScienceDirect

Energy

journal homepage: www.elsevier.com/locate/energy

High-performance energy storage of poly (o-methoxyaniline) film using an ionic liquid as electrolyte

W.A. Christinelli, L.G. da Trindade, A.B. Trench, C.S. Quintans, C.M. Paranhos, E.C. Pereira*

Chemistry Dept., Federal University of São Carlos, C.P. 676, 13560-970, São Carlos, SP, Brazil

ARTICLE INFO

Article history:
Received 22 June 2017
Received in revised form
24 August 2017
Accepted 5 November 2017
Available online 7 November 2017

Keywords:
Conducting polymers
Poly (o-methoxyaniline)
Supercapacitors
Ionic liquid

ABSTRACT

Different materials have been proposed as active electrode in electrochemical capacitors, including conducting polymers. Among them, several papers describe the use of polyaniline and its derivatives for such purpose. However, the use of poly(o-methoxyaniline), a polyaniline derivative, in ionic liquid electrolytes as pseudocapacitors has never been proposed in the literature. Therefore, the objective of this work is to investigate the electrochemical properties and stability of POMA casting film in ionic liquid electrolyte as electrode for supercapacitors. Cyclic voltammetry and galvanostatic charge/discharge experiments have been used to analyze the behavior of the films. The results show that POMA films have high specific capacitance and good electrochemical stability during 3000 cycles. Its initial value is 260 F g^{-1} in a mixture of ionic liquid and polyethylene glycol (80:20 v/v). The specific energy shows 70% retention from the initial value after 3000 cycles. Furthermore, the specific power remains remarkably stable during 3000 cycles, as well as the coulombic efficiency, which is about 99%. For these reasons this work opens up the possibilities of using conducting polymers in ionic liquids and illustrates its good behavior and stability for supercapacitor application.

1. Introduction

Since their discovery, more than three decades ago, conducting polymers (CPs) have received a lot of attention involving the basic aspects of their behavior as well as their use to build different devices for technological applications. The number of papers published in scientific literature about these materials has grown significantly due to their great versatility in application [1,2]. Starting at the 90's, several studies of the properties of CPs have been reported looking for their technological applications. Among them, one of the most promising has been the use of the poly(*p*-Phenylene Vinylene), PPV, for light emitting diodes proposed by Burroughes et al. [3]. Since then, the conducting polymers have be effectively employed in different applications such as: electrochemical batteries [4–7], supercapacitors [8–12], electrochromic devices [13–17] and sensors [18–22].

Among the electrochemical devices, supercapacitors have been extensively explored as promising energy storage [23–29]. Supercapacitors have fundamentally the same principles of a conventional capacitor and can been divided in two kinds according to the mechanism of charge storage: Electrical double layer supercapacitor (EDLCs) and electrochemical capacitors. In EDLCs, there is no electron transfer thorough the interface and the capacitance arises from the charge accumulation at the electrode/electrolyte interface. Electrochemical capacitors are based on faradaic reactions of the electrode, then, there is a charge transfer at the interface. The energy storage occurs during the charge and discharge processes. The later devices are interesting because they present higher capacity per gram than EDLCs. Among the materials investigated as supercapacitor electrodes, conducting polymers are the most promising as they possess good electrical conductivity, redox pseudocapacitance in addition to double layer capacitance, and low cost [30–32].

One of the conducting polymers that has been receiving much attention to be used into supercapacitors is polyaniline (PANI) which has a good chemical stability and low cost. Despite the numerous advantages of PANI, its use is limited because it is insoluble in common solvents. Due to this aspect, it is proposed the substitution of the aromatic ring of aniline with electron donating groups to improve its solubility. In this sense, poly (o-methoxyaniline) (POMA) presents good processability associated with similar electrochemical and electronic behavior of PANI. These

* Corresponding author.
E-mail address: ernesto@ufscar.br (E.C. Pereira).

https://doi.org/10.1016/j.energy.2017.11.026
0360-5442/

materials can be positively charged (p-doped polymer) and the double layer capacitance along with the pseudocapacitance contribute to the total capacitance [33–35].

Supercapacitor devices are usually built using liquid electrolytes (both aqueous and/or organic) [36,37]. In this regard, many papers have focused on the use of ionic liquids (IL's) as impregnating electrolyte for electrochemical supercapacitors, with the purpose of increasing its energy density [38–40]. Liew et al. [41] evaluated the performance of 1-butyl-3-methylimidazolium iodide (BmImI) ionic liquid and ammonium acetate (CH_3COONH_4) added PVA (poly (vinyl alcohol))-based ion conductors for EDLCs using electrochemical measurements. The authors observed that the addition of ionic liquid can enhance the electrochemical stability of polymer electrolytes with the operational current higher than liquid-free polymer electrolyte. The specific capacitance increase of 0.14 F g^{-1} to 52.8 F g^{-1} with the IL addition, this increase of capacitance was attributed to high ionic conductivity of polymer electrolyte. Life cycle tests were carried out to determine the stability of the cell at high charging and discharging cycles. After 500 cycles, the coulombic efficiency of the EDLC with IL maintain the capacitance above 80% of its initial value. The energy density and power density of the cell drop gradually from first cycle to 200th cycles, however, these values almost remain unchanged above the 300th cycles. These compounds, IL's, are salts that have a melting point below 100 °C and low vapor pressure, comprising ions and characterized by low reticular energy due to the combination of a large cation with a delocalized charge anion. These substances exhibit good ionic conductivity and wide electrochemical window stability [42,43].

Moreover, using ILs as electrolyte allows also the electrolyte composition optimization to meet adequate performance requirements for supercapacitors as operating cell voltage, and temperature range. The dilution of IL's in secondary solvent decreases the solution viscosity and increases the ionic conductivity since the ions solvated. In this sense, polyethylene glycol (PEG) is a good alternative due to its low cost and high processability. Furthermore, ethylene glycol has been used in many other applications such as a catalyst, supporting electrolyte, and as stabilizer [37].

Considering that literature about the conducting polymer using ionic liquid as electrolyte are limited to a few studies [44–46], and only one paper describing POMA/IL electrolyte interface has been found [34], this work describes the electrochemical performance of poly (*o*-methoxy aniline) film prepared by *casting* technique in ionic liquid electrolyte. The ionic liquid 1-butyl-3-methylimidazolium tetrafluoroborate ($BMI.BF_4$) was used in different concentrations in a mixture with polyethylene glycol (PEG).

2. Experimental

2.1. Materials and methods

The poly(*o*-methoxy aniline), also known as anisidine, has been synthesized by chemical direct oxidation of the monomer as described by Mattoso [35]. The POMA solution was prepared by dissolving 20 mg of POMA in a mixture of H_2O and acetonitrile (ACN) (J. T. Baker) in a proportion of 59:1 (v/v). ACN was used to enhance the solubility of the polymer in water. All the reactants were supplied by Sigma-Aldrich, and anisidine monomer was purified by distillation under vacuum.

POMA electrodes were prepared by *casting* POMA from the solution onto glass substrates covered with indium tin oxide (ITO) (area = 1 cm^2). These substrates were previously etched with a $H_2O_2/NH_4OH/H_2O$ [1:1:5 (v/v)] solution and ultrapure water (Milli-Q system) to prepare a hydrophilic surface. 250 μL of POMA solution were deposited on ITO electrode leading of polymeric film with of 3.6 10^{-5} g.

1-Butyl-3-methylimidazolium tetrafluoroborate ($BMI.BF_4$) ionic liquid was synthesized as previously described [47,48].

2.2. Characterization

The films were characterized by visible spectroscopy using UV–VIS–NIR spectrophotometer (Cary model 5G) and attenuated total reflectance Fourier transform infrared (ATR-FTIR) spectra using Varian 640-IR FTIR spectrometer in the scanning range of 4000–600 cm^{-1}. The film morphologies were studied using Field Emission Gun - Scanning Electron Microscopy (FEG-SEM) micrographs (ZEISS model 105 DSM940A) working at 10 keV.

Electrochemical experiments were carried out in a three-electrode glass cell using an Autolab PGSTAT 302 N. The measurements were performed in different proportions of ionic liquid in polyethylene glycol (PEG). As a reference and auxiliary electrodes, an Ag pseudo-reference electrode and Pt sheet (area = 1 cm^2) were used, respectively. The electrochemical stability of the electrode has been studied using galvanostatic, and cyclic voltammetry. All measurements were carried out at room temperature in different proportions of ionic liquid in PEG. Galvanostatic charge/discharge cycling, the load current was 4.5 A g^{-1}. Cyclic voltammetry characteristics of films were recorded after each 100 cycles of charge/discharge cycles at 20 mV s^{-1} from −0.2–0.3 V versus Ag.

Besides, the stability tests were also investigated using ATR-FTIR, FEG-SEM, and contact angle (Ramé-Hart Model 21AC Standard Goniometer) measurements.

3. Results and discussions

Fig. 1a present UV–VIS measurements, that exhibit a typical absorption peak around 450 nm due to the polaron bands indicating the formation of the emeraldine salt doped state of POMA in agreement with literature [35,49]. The voltametric behavior of POMA in pure ionic liquid, Fig. 1b, presents one redox couple located between 0 and 0.1 V attributed to the redox transition of POMA between a semiconducting state (leucoemeraldine form) and a conducting state (polaronic emeraldine form), which results is in agreement to literature [50].

The FTIR spectrum of POMA, Fig. 2a, shows the peaks characteristic of POMA [51,52]. The peaks appeared at, 1146, 1218, 1425 cm^{-1} and 1715 cm^{-1}, and could be attributed to C–H out of plane bending vibration, C–N stretching vibrating modes for benzenoid and quinoid rings of primary aromatic amines, C=N (or) C=C stretching modes in the aromatic compounds, respectively. The presence of $-OCH_3$ group in POMA is related to the peak 1218 cm^{-1}. The peaks between 800 and 600 cm^{-1} reveal the occurrence of 1, 2- substitution on aromatic ring.

The vibrational spectrum of $BMI.BF_4$ can be observed at Fig. 2b. In brief, the spectrum shows that the peak at 1441 cm^{-1} which is attributed to CH_2 bending and C-aromatic ring, $C-CH_3$ and the side chain $-CH_2-CH_2-CH_2-$ groups are related to 1550, 1441 and 734 cm^{-1}, respectively. All those bands are associated with $[BMI]^+$. The peaks at 1037 cm^{-1} is attributed to the stretching vibration of B–F bands of $[BF_4]^-$. Finally, the FTIR spectrum of PEG, Fig. 2c, is characterized by the O–H bending vibration at 1307 cm^{-1}, the deformation vibration of the C–H bonds at 1438 and 1380 cm^{-1}, the bending vibration of the O–H at 1234 and 1178 cm^{-1} and the C–O stretching vibration between 1100 and 1000 cm^{-1}. Both, $BMI.BF_4$ and PEG spectra are agreement with the literature [53–55].

The electrochemical behavior of the POMA in different concentrations of ionic liquid in polyethylene glycol are presented in

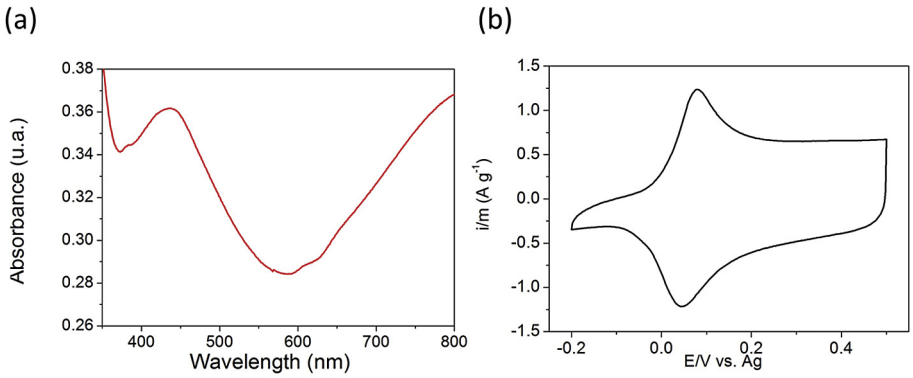

Fig. 1. (a) UV–VIS spectra and (b) Cyclic voltammogram of POMA *casting* film on ITO substrates. Measurements were made in pure ionic liquid at 20 mV s^{-1} at 25 °C.

Fig. 3a. Fig. 3a presents the cyclic voltammograms (CV) of POMA in 20, 40, 60 e 80% of ionic liquid using PEG as solvent. Analyzing Fig. 3a, it is possible to observe that the CV profile of POMA changes with the concentration of ionic liquid in the solvent. The proportions from 20 to 60% of IL in PEG show a capacitive CV fingerprint, while, for pure ionic liquid electrolyte, the voltammetric profile is neatly faradaic. Moreover, an increase in the specific current for 80% IL in PEG can be observed. As a consequence, the specific capacitance values calculated from the voltammetric curves present the same kind of behavior. The calculated values are close to 170 F g^{-1} up to 60% IL and it increases to 236 F g^{-1} for the solution 80% IL. The relatively low values of specific capacitance observed for 20–60% IL in PEG could be attributed to small amounts of ionic species in the medium reflecting in the specific capacitance values. In the same way, for 100% IL, the specific capacitance is low duo to the strong interactions between the BMI^+ and BF_4^- leading to a decrease in the ionic conductivity. The high value observed for 80% IL/PEG, which corresponds to a molar fraction (xBMI.BF_4) of 0.50, could be explained by the solvation of IL in PEG and the solution viscosity [56]. Silva et al. [56] studied the solvent effects on electrolyte transport properties of BMI.BF_4 binary solutions with PEG. The authors found that the maximum ionic conductivity values is observed for xBMI.BF_4 0.50 at room temperature and attributed this results to two factors: the break of the strong coulombic interactions and solvation of ions BMI^+ and BF_4^-, suggesting that the ionic conductivity is not only related to the viscosity but also to the ion-ion, ion-solvent and solvent-solvent interactions.

In order to further understand the high value of specific capacitance for 80% IL/PEG we carried out galvanostatic charge/discharge measurements. Fig. 4a presents the charge/discharge curves at different current densities for POMA *casting* film. All of them exhibit two charge/discharge stages in the potential-time curve: 0.3 to 0 and 0 to −0.2 V, respectively. The first stage could be attributed to the electric double-layer capacitance of the electrode [49]. During the later stage, the combination of electric double-layer capacitance and Faradaic capacitance could be responsible for the charge/discharge duration [57]. This change in the slope of the curve occurs at the same region in the voltammograms where the oxidation (reduction) potential peak occurs due to the intercalation (deintercalation) process (Fig. 3a) [23,57,58]. Analysing the specific capacitance (Fig. 4b) calculated from charge/discharge curves, it can be observed that the specific capacitance values decrease as the applied current density increase. These results are an indication that the ion diffusion resistance is higher as the applied current density is increased. The values for the calculated ohmic drop (IR drop) are presented in Table 1.

Fig. 4c presents both the amount of energy and the specific

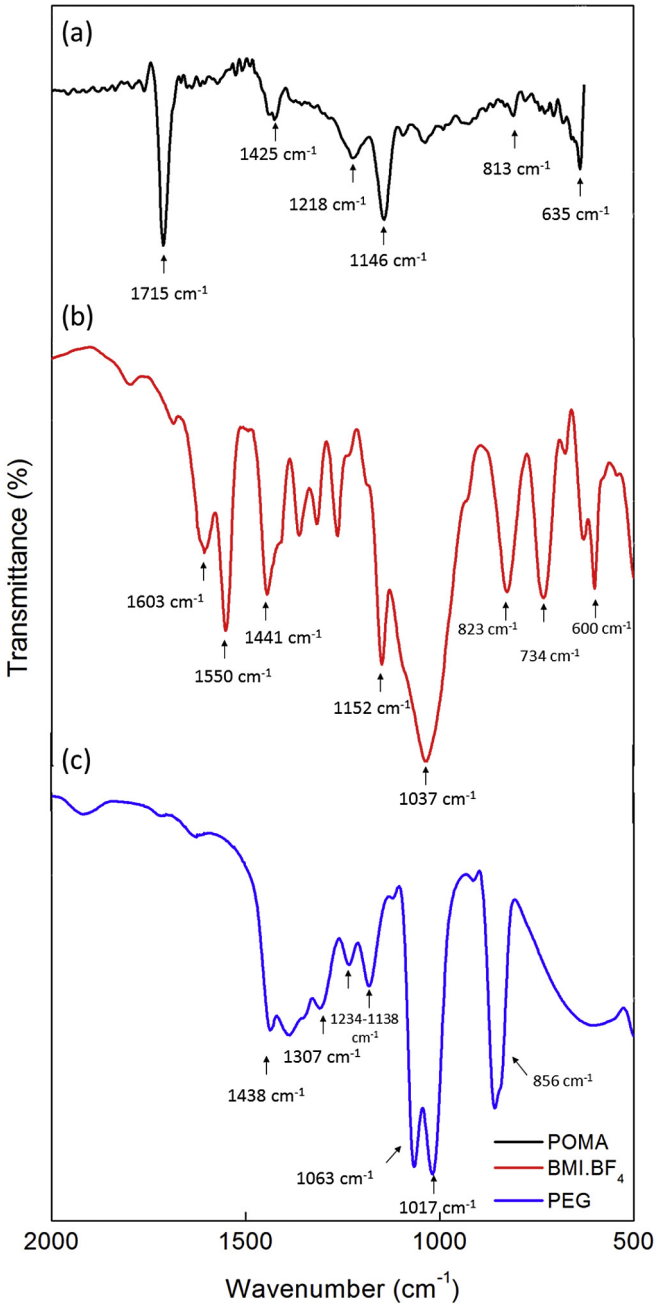

Fig. 2. ATR-FTIR spectra of (a) POMA casting film (b) BMI.BF_4 and (c) PEG.

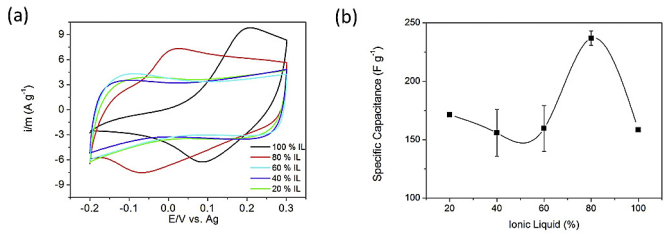

Fig. 3. (a) Cyclic voltammogram and (b) Specific capacitance of POMA film in different proportions of ionic liquid in PEG. Measurements were made at 20 mV s^{-1} at 25 °C.

power that is stored in this material normalized by the active mass. According to Snook [31] and, more recently, to Abdelhamid [30], conducting polymer-based supercapacitors devices are designed to be a bridge in the gap between the existing capacitors and batteries. Then they are materials have intermediate specific energy and high specific power. Analysing Fig. 4c, it can be observed that the values of specific energy and power are about 3.6 Wh kg^{-1} and 800 W kg^{-1}, respectively which are close to those values described for different supercapacitors in literature showing that POMA *casting* films are promising materials for supercapacitor application.

For technological applications, not only a high specific capacitance, intermediate specific energy and high specific power are necessary. A high cyclability is also required, i.e., electrochemical aging stability. Analyzing those data in Fig. 4, we choose to investigate the electrochemical aging of the films using galvanostatic charge/discharge experiments at a current density of 4.5 A g^{-1} and a potential range between −0.2 V and 0.3 V (vs. Ag). Fig. 5a and b presented the galvanostatic charge/discharge curves and the cyclic voltammetries before and after 3000 cycles of aging process. As can be observed in Fig. 5a, there is a small change in the slope of the discharge part of the curve after 3000 cycles. Besides, the CV profiles (Fig. 5b) presents similar behavior during the aging process.

Using the data in Fig. 5, the specific capacitance based on POMA as a function of number of cycles are presented in Fig. 6. The conducting polymer material electrode exhibited excellent stability over the entire aging experiment. The specific capacitance at the beginning of charge/discharge measurement was 260 F g^{-1} and, after 3000 cycles, this value falls down to 157 F g^{-1}. These results indicate that the specific capacitance retention of POMA is 60.5% after 3000 cycles. It is important to stress that the most significant change in the specific capacitance occurs during the first 1000 cycles. After that, the value of SC falls down additionally only 15%.

Furthermore, we investigate the specific energy, specific power and the coulombic efficiency during the long-term cycling stability of POMA which are shown in Fig. 7. The energy (Fig. 7a, black squares) at the beginning of aging process is 3.7 Wh Kg^{-1} and, after 3000 cycles, the value drops down to 2.6 Wh Kg^{-1}, which means a 70% of energy retention. The specific power (Fig. 7a) remains

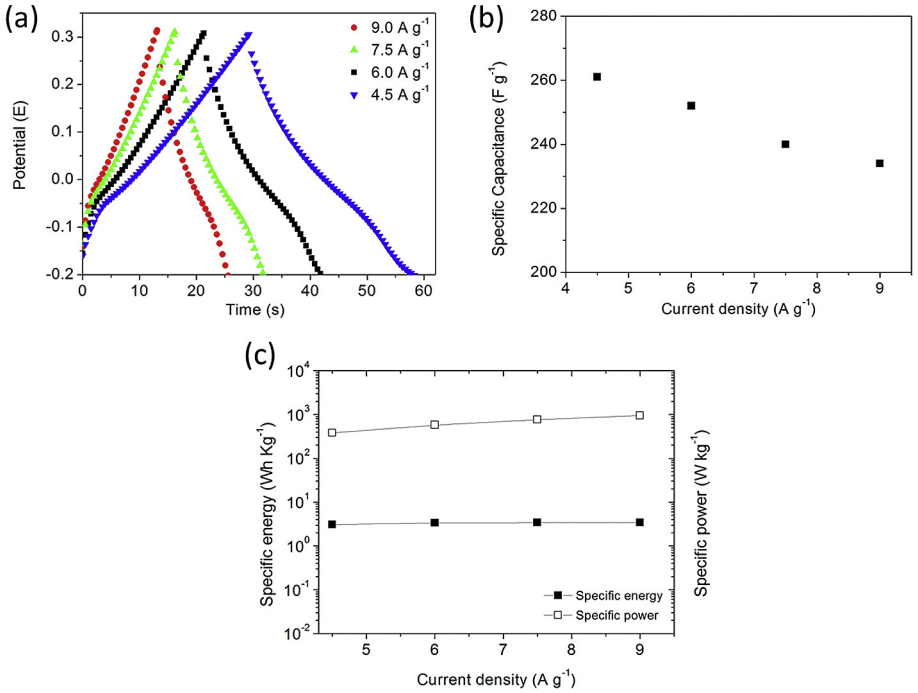

Fig. 4. Charge/Dicharge characterization of POMA cast film in solution of 80% IL. (a) Charge-discharge profiles from −0.2 V to 0.3 V, (b) specific capacitance, (c) specific energy and power obtained from CD profiles at different current densities at 25 °C.

Table 1
IR drop, specific capacitance, specific energy and specific power values at different current densities.

Current density (A g^{-1})	IR drop (V)	Specific Capacitance (F g^{-1})	Specific Energy (Wh Kg^{-1})	Specific Power (W Kg^{-1})
4.5	0.041	261	3.063	380.270
6.0	0.052	252	3.378	579.138
7.5	0.064	240	3.413	768.030
9.0	0.077	234	3.435	951.397

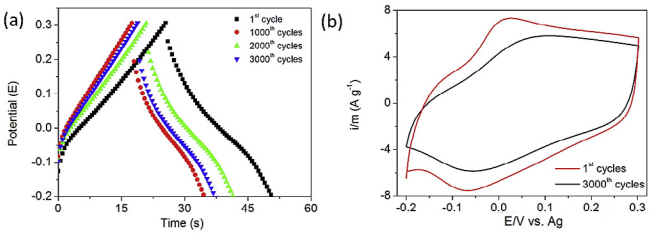

Fig. 5. (a) Charge-discharge profiles from −0.2 V to 0.3 V, (b) Cyclic voltammogram for POMA cast film during 3000 cycles in solution of 80% IL.

remarkably stable during 3000 cycles, as well as the coulombic efficiency (Fig. 7b). The coulombic efficiency of POMA film retained nearby of 99% indicating an excellent reversibility of the process. In conclusion, all the results together allow us to propose that POMA casting films in IL are a promising material for supercapacitor application.

A complete description of the degradation process of POMA in ionic liquid + PEG is beyond the scope of this work, but some hypothesis to explain the obtained behavior can be proposed. Fig. 8 presents the IR spectra, contact angle FEG-SEM images for flash and electrochemical aged samples.

From the FTIR spectra, Fig. 8a, we can observed that, after 3000 cycles, the appearance of a band at 1037 cm^{-1} which could be attributed to the stretching vibration of B–F bands of BF_4^- anion of IL. It is also important to consider that both ions of the ionic liquid are large and there is a low probability that these ions can intercalate in the polymers chains as occurs for POMA investigated in common salts, such as $LiClO_4$ [12]. In those work [12], investigating POMA casting samples, it was observed an important degradation during electrochemical aging measurements in 0.1 M $LiClO_4$ acetonitrile solution. It was found that POMA samples presents a continuous degradation as the number of aging cycles are increased resulting in an 80% decrease from the initial specific capacitance value after 3000 cycles. It is well established that in conducting polymers, the oxidation (reduction) processes leads to the intercalation (deintercalation) of counter ions to compensate the generated charge in the material. Several papers [30,31,59] in the literature attribute such decrease to a reversible change in the polymer volume at each redox cycles. This change is associated to the large volume of the solvated ions when they intercalate. In the present case, considering the large volume of the ions of the ionic liquid, a much more severe effect on the electrochemical deactivation could be expected if these ions intercalate into the polymer. As can be observed in Figs. 6–8, such decrease does not occur, although there is a large amount of ions from the ionic liquid on the sample.

In a second experiment, Fig. 8b, we measured the contact angle of the ionic liquid on the sample. Contac angle measurements are widely employed to determine indirectly solid-liquid interfacial tensions. It is well known, from Young's approach, that the total surface tensions can be expressed as the sum of dispersive and non-dispersive intermolecular forces components [60]. Interestingly the PEG:$BMI.BF_4$ (80%) electrolyte contact angle of the polymer in the first cycle was not significantly different (26.4°) than that of the value measured after the 3000 cycles (29.6°), indicating that surface wettability does not changed after 3000 cycles [61]. Then, it is possible to propose that there is not any important change in the polymer wettability which indicates also there is not any charge accumulation in the material or important material degradation. Finally, we measured images from the sample surface using FEG-SEM technique (Fig. 8c). Again, it was not observed any significant change in the surface morphology. In a previous work, for those samples where an electrochemical degradation occurs, there is important change comparing flash and aged POMA samples [12]. Then, the result here presented at Fig. 8c is an indication that a degradation does not occurs, in agreement for those data from Figs. 6 and 7. Then, considering all the results and comparing with those previously published one possible explanation for these results is the absence of intercalation of counter ions into the polymer

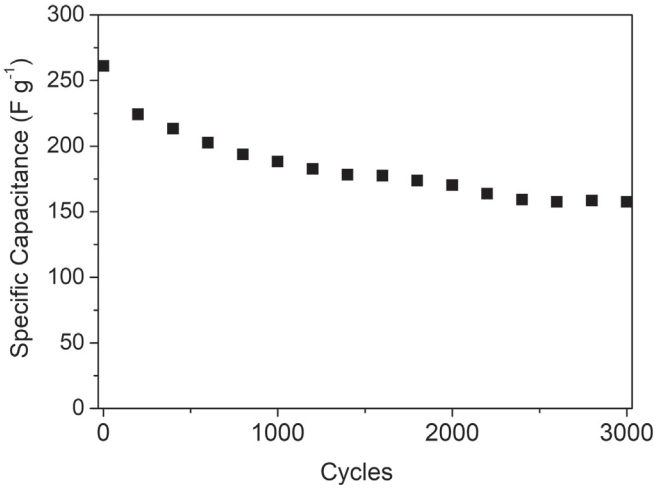

Fig. 6. Specific capacitance aging for POMA *casting* film during 3000 cycles of charge/discharge measurements in solution of 80% IL.

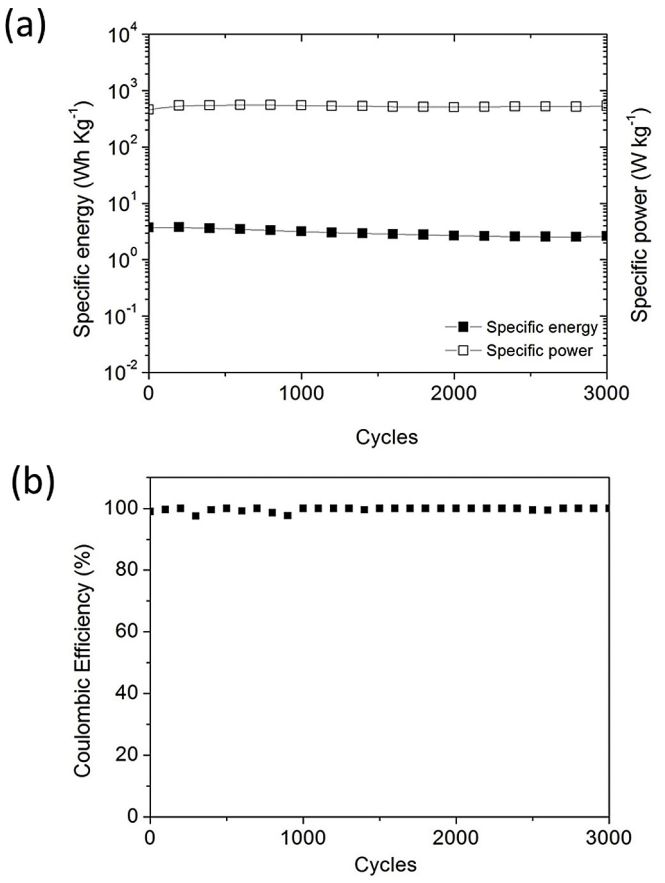

Fig. 7. Charge/Dicharge characterization of POMA cast film. (a) specific energy and power and (b) Coulombic efficiency during 3000 cycles in solution of 80% IL.

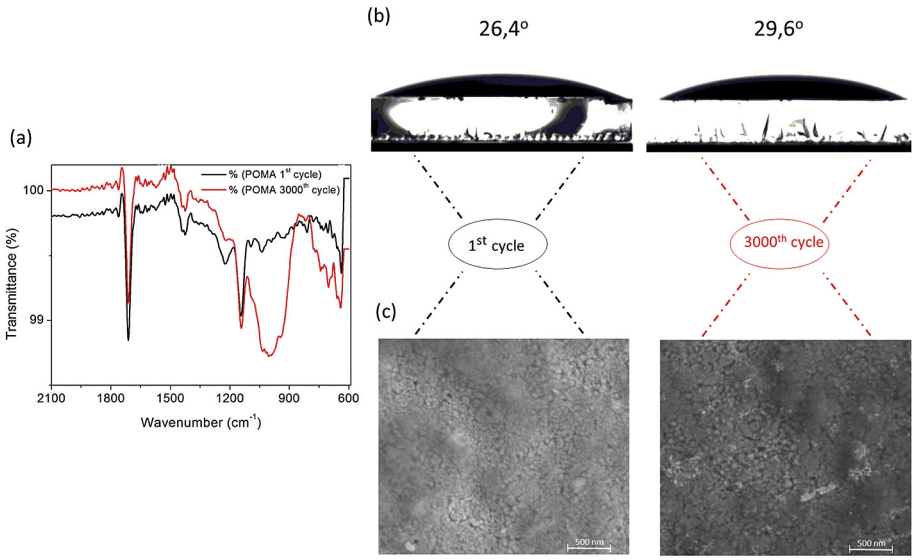

Fig. 8. (a) FTIR spectra, (b) contact angles and (c) SEM micrographs of POMA at 1st cycle and 3000th cycle.

chains during the redox process duo to the high size of ions. In other words, the results indicate that the in this case the mechanism of charge accumulation on film appears at the interface between a surface of conducting electrode and an adjacent liquid electrolyte as a double layer effect. The large value obtained for the capacitance could, then, be associated to the large area surface.

4. Conclusions

In this paper, the electrochemical properties of POMA *casting* film in ionic liquid electrolyte have been studied. The results show that POMA films have high specific capacitance, 260 F g^{-1} for 80% of BMI.BF_4 in PEG, and good electrochemical stability during 3000 cycles. The specific energy shows 70% of retention from the initial value and the specific power remains remarkably stable during 3000 cycles, as well as the coulombic efficiency in which retained nearby of 99%. From the data on the literature, this is the first report on conducting polymer films in an ionic liquid and polyethylene glycol electrolyte. The results suggest that charge accumulation is a double layer effect. This work opens up the possibilities of using conducting polymers in ionic liquids and illustrating the good behavior and stability for supercapacitor application.

Acknowledgments

The support of this research by FAPESP (Grant# 2011/10897-2, 2016/05363-2, 2013/07296-2), CAPES and CNPq (Grant# 159387/2015-9) is gratefully acknowledged.

References

[1] Shi Y, Peng L, Ding Y, Zhao Y, Yu G. Nanostructured conductive polymers for advanced energy storage. Chem Soc Rev 2015;44:6684–96. https://doi.org/10.1039/C5CS00362H.
[2] Inzelt G. Rise and rise of conducting polymers. J Solid State Electrochem 2011;15(7–8):1711–8. https://doi.org/10.1007/s10008-011-1338-3.
[3] Burroughes JH, Bradley DDC, Brown ARR, Marks N, Mackay K, Friend RH, et al. Light-emitting diodes based on conjugated polymers. Nature 1990;347(6293):539–41. https://doi.org/10.1038/347539a0.
[4] MacDiarmid AG. A review of conductive polymer batteries. Abstr Pap Am Chem Soc 1983;186. 15–Inde.
[5] Otero TF, Cantero I. Conducting polymers as positive electrodes in rechargeable lithium-ion batteries. J Power Sources 1999;81:838–41. https://doi.org/10.1016/S0378-7753(98)00236-5.
[6] Yang Y, Yu G, Cha JJ, Wu H, Vosgueritchian M, Yao Y, et al. Improving the performance of lithium–sulfur batteries by conductive polymer coating. ACS Nano 2011;5(11):59187–93. https://doi.org/10.1021/nn203436j.
[7] Katz HE, Searson PC, Poehler TO. Batteries and charge storage devices based on electronically conducting polymers. J Mater Res 2010;25(8):1561–74. https://doi.org/10.1557/JMR.2010.0201.
[8] Wang Y, Xia Y. Recent progress in supercapacitors: from materials design to system construction. Adv Mater 2013;25(37):5336–42. https://doi.org/10.1002/adma.201301932.
[9] Frackowiak E, Khomenko V, Jurewicz K, Lota K, Béguin F. Supercapacitors based on conducting polymers/nanotubes composites. J Power Sources 2006;153(2):413–8. https://doi.org/10.1016/j.jpowsour.2005.05.030.
[10] Arbizzani C, Mastragostino M, Meneghello L. Polymer-based redox supercapacitors: a comparative study. Electrochim Acta 1996;41(1):21–6. https://doi.org/10.1016/0013-4686(95)00289-Q.
[11] Christinelli WA, Gonçalves R, Pereira EC. A new generation of electrochemical supercapacitors based on layer-by-layer polymer films. J Power Sources 2016;303:73–80. https://doi.org/10.1016/j.jpowsour.2015.10.077.
[12] Christinelli WA, Gonçalves R, Pereira EC. Optimization of electrochemical capacitor stability of poly(o-methoxyaniline)-poly(3-thiophene acetic acid) self-assembled films. Electrochim Acta 2016;196:741–8. https://doi.org/10.1016/j.electacta.2016.02.187.
[13] Ram MK, Maccioni E, Nicolini C. The electrochromic response of polyaniline and its copolymeric systems. Thin Solid Films 1997;303(1–2):27–33. https://doi.org/10.1016/S0040-6090(97)00068-0.
[14] Patil RA, Devan RS, Lin J-H, Ma Y-R, Patil PS, Liou Y. Efficient electrochromic properties of high-density and large-area arrays of one-dimensional NiO nanorods. Sol Energy Mater Sol Cells 2013;112:91–6. https://doi.org/10.1016/j.solmat.2013.01.003.
[15] Giglioti M, Trivinho-Strixino F, Matsushima JT, Bulhões LOS, Pereira EC. Electrochemical and electrochromic response of poly(thiophene-3-acetic acid) films. Sol Energy Mater Sol Cells 2004;82(3):413–20. https://doi.org/10.1016/j.solmat.2004.02.001.
[16] Christinelli WA, Trench AB, Pereira EC. Electrochromic properties of poly(o-methoxyaniline)-poly(3-thiophene acetic acid) layer by layer films. Sol Energy Mater Sol Cells 2016;157:703–8. https://doi.org/10.1016/j.solmat.2016.07.035.
[17] Yang P, Sun P, Mai W. Electrochromic energy storage devices. Mater Today 2016;19(7):394–402. https://doi.org/10.1016/j.mattod.2015.11.007.
[18] Lange U, Roznyatovskaya NV, Mirsky VM. Conducting polymers in chemical sensors and arrays. Anal Chim Acta 2008;614(1):1–26. https://doi.org/10.1016/j.aca.2008.02.068.
[19] Pereira NS, Sales MJA, Ceschin AM. Study of the interactions between POMA/PMMA blends with pesticide atrazine: potential application in sensors. Sens Lett 2011;9(2):675–8. https://doi.org/10.1166/sl.2011.1589.
[20] Correa DS, Medeiros ES, Oliveira JE, Paterno LG, Mattoso LHC. Nanostructured conjugated polymers in chemical sensors: synthesis, properties and applications. J Nanosci Nanotechnol 2014;14(9):6509–27. https://doi.org/10.1166/jnn.2014.9362.
[21] Riul A, Malmegrim RR, Fonseca FJ, Mattoso LHC. An artificial taste sensor based on conducting polymers. Biosens Bioelectron 2003;18(11):1365–9. https://doi.org/10.1016/S0956-5663(03)00069-1.
[22] Nambiar S, Yeow JTW. Conductive polymer-based sensors for biomedical applications. Biosens Bioelectron 2011;26(5):1825–32. https://doi.org/10.1016/j.bios.2010.09.046.

[23] Bryan AM, Santino LM, Lu Y, Acharya S, D'Arcy JM. Conducting polymers for pseudocapacitive energy storage. Chem Mater 2016;28(17):5989–98. https://doi.org/10.1021/acs.chemmater.6b01762.

[24] Xia X, Zhang Y, Chao D, Xiong Q, Fan Z, Tong X, et al. Tubular TiC fibre nanostructures as supercapacitor electrode materials with stable cycling life and wide-temperature performance. Energy Environ Sci 2015;8:1559–68. https://doi.org/10.1039/C5EE00339C.

[25] Xia X, Zhang Y, Chao D, Xiong Q, Fan Z, Tong X, et al. Generic synthesis of carbon nanotube branches on metal oxide arrays exhibiting stable high-rate and long-cycle sodium-ion storage. Small 2016;12:3048–58. https://doi.org/10.1002/smll.201600633.

[26] Zhong Y, Xia X, Shi F, Zhan J, Tu J, Fan HJ. Transition metal carbides and nitrides in energy storage and conversion. Adv Sci 2016;3(5):1500286–313. https://doi.org/10.1002/advs.201500286.

[27] Weingarth D. Ionic liquids for electrochemical double layer capacitors. In: Department of chemistry and applied biosciences. ETH: Zürich; 2013. https://doi.org/10.3929/ethz-a-009900708.

[28] Yanik MO, Yigit EA, Akansu YE, Sahmetlioglu E. Magnetic conductive polymer-graphene nanocomposites based supercapacitors for energy storage. Energy 2017;138:883–9. https://doi.org/10.1016/j.energy.2017.07.022.

[29] Tehrani Z, Thomas DJ, Korochkina T, Phillips CO, Lupo D, Lehtimäki S, et al. Large-area printed supercapacitor technology for low-cost domestic green energy storage. Energy 2017;118:1313–21. https://doi.org/10.1016/j.energy.2016.11.019.

[30] Abdelhamid ME, O'Mullane AP, Snook GA. Storing energy in plastics: a review on conducting polymers and their role in electrochemical energy storage. RSC Adv 2015;5:11611–26. https://doi.org/10.1039/C4RA15947K.

[31] Snook GA, Kao P, Best AS. Conducting-polymer-based supercapacitor devices and electrodes. J Power Sources 2011;196(1):1–12. https://doi.org/10.1016/j.jpowsour.2010.06.084.

[32] Lee S-Y, Kim J-I, Park S-J. Activated carbon nanotubes/polyaniline composites as supercapacitor electrodes. Energy 2014;78:298–303. https://doi.org/10.1016/j.energy.2014.10.011.

[33] Yang X, Wang G, Wang R, Li X. A novel layered manganese oxide/poly(aniline-co-o-anisidine) nanocomposite and its application for electrochemical supercapacitor. Electrochim Acta 2010;55(19):5414–9. https://doi.org/10.1016/j.electacta.2010.04.067.

[34] Basnayaka PA, Ram MK, Stefanakos L, Kumar A. High performance graphene-poly (o-anisidine) nanocomposite for supercapacitor applications. Mater Chem Phys 2013;141(1):263–71. https://doi.org/10.1016/j.matchemphys.2013.05.009.

[35] Mattoso LHC, MacDiarmid AG, Epstein AJ. Controlled synthesis of high molecular weight polyaniline and poly(o-methoxyaniline). Synth Met 1994;68(1):1–11. https://doi.org/10.1016/0379-6779(94)90140-6.

[36] Zhang L, Tsay K, Bock C, Zhang J. Ionic liquids as electrolytes for non-aqueous solutions electrochemical supercapacitors in a temperature range of 20°C–80°C. J Power Sources 2016;324:615–24. https://doi.org/10.1016/j.jpowsour.2016.05.008.

[37] Ramasamy C, Palma del Val J, Anderson M. An analysis of ethylene glycol-aqueous based electrolyte system for supercapacitor applications. J Power Sources 2014;248:370–7. https://doi.org/10.1016/j.jpowsour.2013.09.078.

[38] Lewandowski A. Electrochemical capacitors with polymer electrolytes based on ionic liquids. Solid State Ionics 2003;161(3–4):243–9. https://doi.org/10.1016/S0167-2738(03)00275-3.

[39] Chen Y, Zhang X, Zhang D, Yu P, Ma Y. High performance supercapacitors based on reduced graphene oxide in aqueous and ionic liquid electrolytes. Carbon N Y 2011;49(2):573–80. https://doi.org/10.1016/j.carbon.2010.09.060.

[40] Biso M, Mastragostino M, Montanino M, Passerini S, Soavi F. Electropolymerization of poly(3-methylthiophene) in pyrrolidinium-based ionic liquids for hybrid supercapacitors. Electrochim Acta 2008;53(27):7967–71. https://doi.org/10.1016/j.electacta.2008.06.008.

[41] Liew C-W, Ramesh S, Arof AK. Enhanced capacitance of EDLCs (electrical double layer capacitors) based on ionic liquid-added polymer electrolytes. Energy 2016;109:546–56. https://doi.org/10.1016/j.energy.2016.05.019.

[42] Galiński M, Lewandowski A, Stępniak I. Ionic liquids as electrolytes. Electrochim Acta 2006;51(26):5567–80. https://doi.org/10.1016/j.electacta.2006.03.016.

[43] Armand M, Endres F, MacFarlane DR, Ohno H, Scrosati B. Ionic-liquid materials for the electrochemical challenges of the future. Nat Mater 2009;8:621–9. https://doi.org/10.1038/nmat2448.

[44] Trchová M, Šeděnková I, Morávková Z, Stejskal J. Conducting polymer and ionic liquid: improved thermal stability of the material – a spectroscopic study. Polym Degrad Stab 2014;109:27–32. https://doi.org/10.1016/j.polymdegradstab.2014.06.012.

[45] Brooke R, Fabretto M, Krasowska M, Talemi P, Pering S, Murphy PJ, et al. Organic energy devices from ionic liquids and conducting polymers. J Mater Chem C 2016;4:1550–6. https://doi.org/10.1039/C5TC03281D.

[46] Li X, Liu Y, Guo W, Chen J, He W, Peng F. Synthesis of spherical PANI particles via chemical polymerization in ionic liquid for high-performance supercapacitors. Electrochim Acta 2014;135:550–7. https://doi.org/10.1016/j.electacta.2014.05.051.

[47] Dupont J, Consorti CS, Suarez PAZ, de Souza RF. Preparation of 1-butyl-3-methyl imidazolium-based room temperature ionic liquids. Org Synth 2002;79:236–9. https://doi.org/10.15227/orgsyn.079.0236.

[48] Suarez PAZ, Dullius JEL, Einloft S, de Souza RF, Dupont J. The use of new ionic liquids in two-phase catalytic hydrogenation reaction by rhodium complexes. Polyhedron 1996;15(7):1217–9. https://doi.org/10.1016/0277-5387(95)00365-7.

[49] Malinauskas A. Self-doped polyanilines. J Power Sources 2004;126(1–2):214–20. https://doi.org/10.1016/j.jpowsour.2003.08.008.

[50] Ćirić-Marjanović G. Recent advances in polyaniline research: polymerization mechanisms, structural aspects, properties and applications. Synth Met 2013;177:1–47. https://doi.org/10.1016/j.synthmet.2013.06.004.

[51] Pramodini S, Poornesh P. Continuous wave laser induced third-order nonlinear optical properties of conducting polymers. Polym Eng Sci 2015;55(10):2396–402. https://doi.org/10.1002/pen.24128.

[52] Pawar P, Gaikwad AB, Patil PP. Corrosion protection aspects of electrochemically synthesized poly(o-anisidine-co-o-toluidine) coatings on copper. Electrochim Acta 2007;52(19):5958–67. https://doi.org/10.1016/j.electacta.2007.03.043.

[53] Tamilarasan P, Mishra AK, Ramaprabhu S. Graphene/ionic liquid binary electrode material for high performance supercapacitor. In: International conference on nanoscience, technology and societal implications; 2011. p. 1–5. https://doi.org/10.1109/NSTSI.2011.6111793.

[54] Wu J, Wang MJ, Stark JPW. Evaluation of band structure and concentration of ionic liquid $BMImBF_4$ in molecular mixtures by using second derivatives of FTIR spectra. J Quant Spectrosc Radiat Transf 2006;102(2):228–35. https://doi.org/10.1016/j.jqsrt.2006.02.009.

[55] Wang C, Feng L, Yang H, Xin G, Li W, Zheng J, et al. Graphene oxide stabilized polyethylene glycol for heat storage. Phys Chem Chem Phys 2012;14:13233–8. https://doi.org/10.1039/c2cp41988b.

[56] da Silva FT, Lima DW, Becker MR, de Souza RF, Martini EMA. Transport properties of binary solutions containing the ionic liquid $BMI.BF_4$ and ethylene glycol. J Braz Chem Soc 2015;26(10):2125–9.

[57] Brousse T, Belanger D, Long JW. To Be or not to Be pseudocapacitive? J Electrochem Soc 2015;162(5):A5185–9. https://doi.org/10.1149/2.0201505jes.

[58] Simon P, Gogotsi Y, Dunn B. Where do batteries end and supercapacitors begin? Science 2014;343(6176):1210–1. https://doi.org/10.1126/science.1249625.

[59] Otero TF, Martinez JG, Arias-Pardilla J. Biomimetic electrochemistry from conducting polymers. A review Artificial muscles, smart membranes, smart drug delivery and computer/neuron interfaces. Electrochim Acta 2012;84:112–28. https://doi.org/10.1016/j.electacta.2012.03.097.

[60] Fowkes FM. Attractive forces at interfaces. Ind Eng Chem 1964;56(12):40–52. https://doi.org/10.1021/ie50660a008.

[61] Grundke K, Bogumil T, Gietzelt T, Jacobasch H-J, Kwok DY, Neumann AW. Wetting measurements on smooth, rough and porous solid surfaces. Prog Colloid Polym Sci 1996;101:58–68. https://doi.org/10.1007/BFb0114445.